



OPEN ACCESS

EDITED BY

Wenjie Zhang,
Shanghai Jiao Tong University, China

REVIEWED BY

Wei Qiao,
The University of Hong Kong, Hong Kong SAR,
China
Shaobao Liu,
Nanjing University of Aeronautics and
Astronautics, China
He Xiao-Tao,
Fourth Military Medical University, China

*CORRESPONDENCE

Zhiguo Qu,
✉ zgqu@xjtu.edu.cn
Ang Li,
✉ dliang@xjtu.edu.cn

[†]These authors have contributed equally to this work and share first authorship

RECEIVED 15 December 2023

ACCEPTED 14 March 2024

PUBLISHED 19 April 2024

CITATION

Sun G, Shu T, Ma S, Li M, Qu Z and Li A (2024), A submicron forest-like silicon surface promotes bone regeneration by regulating macrophage polarization. *Front. Bioeng. Biotechnol.* 12:1356158. doi: 10.3389/fbioe.2024.1356158

COPYRIGHT

© 2024 Sun, Shu, Ma, Li, Qu and Li. This is an open-access article distributed under the terms of the [Creative Commons Attribution License \(CC BY\)](https://creativecommons.org/licenses/by/4.0/). The use, distribution or reproduction in other forums is permitted, provided the original author(s) and the copyright owner(s) are credited and that the original publication in this journal is cited, in accordance with accepted academic practice. No use, distribution or reproduction is permitted which does not comply with these terms.

A submicron forest-like silicon surface promotes bone regeneration by regulating macrophage polarization

Guo Sun^{1,2†}, Tianyu Shu^{1†}, Shaoyang Ma¹, Meng Li¹, Zhiguo Qu^{2*} and Ang Li^{1*}

¹Key Laboratory of Shaanxi Province for Craniofacial Precision Medicine Research, College of Stomatology, Xi'an Jiaotong University, Xi'an, China, ²MOE Key Laboratory of Thermo-Fluid Science and Engineering, School of Energy and Power Engineering, Xi'an Jiaotong University, Xi'an, China

Introduction: Silicon is a major trace element in humans and a prospective supporting biomaterial to bone regeneration. Submicron silicon pillars, as a representative surface topography of silicon-based biomaterials, can regulate macrophage and osteoblastic cell responses. However, the design of submicron silicon pillars for promoting bone regeneration still needs to be optimized. In this study, we proposed a submicron forest-like (Fore) silicon surface (Fore) based on photoetching. The smooth (Smo) silicon surface and photoetched regular (Regu) silicon pillar surface were used for comparison in the bone regeneration evaluation.

Methods: Surface parameters were investigated using a field emission scanning electron microscope, atomic force microscope, and contact angle instrument. The regulatory effect of macrophage polarization and succedent osteogenesis was studied using Raw264.7, MC3T3-E1, and rBMSCs. Finally, a mouse calvarial defect model was used for evaluating the promoting effect of bone regeneration on the three surfaces.

Results: The results showed that the Fore surface can increase the expression of M2-polarized markers (CD163 and CD206) and decrease the expression of inflammatory cytokines, including interleukin-6 (IL-6) and tumor necrosis factor alpha (TNF- α). Fore surface can promote the osteogenesis in MC3T3-E1 cells and osteoblastic differentiation of rBMSCs. Furthermore, the volume fraction of new bone and the thickness of trabeculae on the Fore surface were significantly increased, and the expression of RANKL was downregulated. In summary, the upregulation of macrophage M2 polarization on the Fore surface contributed to enhanced osteogenesis *in vitro* and accelerated bone regeneration *in vivo*.

Discussion: This study strengthens our understanding of the topographic design for developing future silicon-based biomaterials.

KEYWORDS

silicon, submicron, surface topography, bone regeneration, macrophage polarization

1 Introduction

The highly efficient restoration of a bone defect is a major clinical concern. The reason is that human bone tissue often shows limited regenerative capacity and requires proper external intervention for regeneration (Bai et al., 2018; Wang X. et al., 2018). Silicon is a major trace element in humans (Jugdaohsingh et al., 2013; Martin, 2013). Increased dietary silicon intake facilitates human skeletal health (Jugdaohsingh et al., 2004). Orthosilicic acid, biosilica, and silica nanoparticles can stimulate type I collagen synthesis and osteoblast differentiation in human osteoblast-like cells (Sun et al., 2017; Sun et al., 2018; Friguglietti et al., 2020). Silicon nitride surfaces have also shown osteogenic/antibacterial dual properties (Bock et al., 2017; Ishikawa et al., 2017; Du et al., 2022). Therefore, silicon shows some potential in stimulating bone regeneration. To develop new silicon-based biomaterials for bone regeneration, the optimized design of bioactive silicon surfaces should be completely elaborated.

The surface topography of biomaterials plays a vital role in osteogenesis (Bosshardt et al., 2017). Installed biomaterials can trigger innate immune responses and recruit macrophages (Trindade et al., 2016). To establish a suitable microenvironment for bone regeneration, the M2-polarized macrophages are necessary with their anti-inflammatory and pro-healing potential to inhibit the innate immune response (Chen et al., 2016; Zhu G. et al., 2021; Toita et al., 2022). It has been proven that proper surface topography of biomaterials can promote the M2 polarization of macrophages to enhance bone regeneration (Hotchkiss et al., 2016; Abaricia et al., 2020; Zhu Y. Z. et al., 2021). In addition, the surface topography of biomaterials can directly influence osteogenesis. That is, the material surface that mimics natural bone topography can promote protein adsorption, mesenchymal stem cell osteogenic differentiation, and trabecular bone ingrowth (Boyan et al., 2017; Shah et al., 2019; Berger et al., 2022). Thus, it is crucial to clarify the regulatory effect of silicon-based biomaterials on macrophage polarization and succedent osteogenesis.

Recently, it was shown that lithography technology shows potential in precisely tailoring the surface topography of biomaterials (Kooy et al., 2014; Brown et al., 2023). Therefore, the surface submicron pillar has been a potential pro-osteogenesis design. Submicron pillars can modulate cell behavior such as adhesion and migration (Nouri-Goushki et al., 2020; Angeloni et al., 2023). Lithographically formed silicon nanorods promote the osteopontin expression in pre-osteoblasts, which reveals its pro-osteogenesis effect (Ganjan et al., 2022). In addition, the density and height of submicron pillars have shown an immunomodulating effect in regulating M1/M2 polarization of macrophages (Nouri-Goushki et al., 2021). Specific submicron pillars (500 nm in diameter and 2 μ m in height) can stimulate macrophage differentiation into osteoclasts (Akasaka et al., 2022). Notably, the submicron silicon pillars in existing studies are dominantly regular. However, the submicron features of human bone (such as lamellae, osteocytes, and the extracellular matrix) are naturally irregular (Shah et al., 2019). The effect of pillar morphology should be considered further when evaluating the biological response of submicron silicon pillars.

Therefore, this study proposes a submicron forest-like (Fore) silicon surface for promoting bone regeneration and compares it with common submicron silicon columns and the smooth (Smo) silicon surface (Figure 1). We investigate the macrophage response and subsequent pro-osteogenesis effect. The *in vivo* bone regeneration

is evaluated in the mouse calvarial defect model. The result will enhance the experimental basis for future silicon-based biomaterial designs.

2 Materials and methods

2.1 Sample preparation and characterization

The Smo, regular (Regu), and Fore submicron silicon surfaces were manufactured by Suzhou Research Materials Microtech Co., Ltd. (China). The Smo surface was a 4,000-grit polished silicon wafer. The Regu surface contained repeating photoetched columns (diameter: 400–500 nm; height: 1,000 nm). The Fore surface contained plasma-treated irregular (diameter: 250–500 nm; height: 800–1,000 nm) pillars. The surface topography was characterized using a field emission scanning electronic microscope (FE-SEM; Hitachi S-4800, Japan). Surface roughness parameters (S_a , S_q , and S_z) were detected using an atomic force microscope (AFM; 5500, Agilent, United States) in a 2.5 mm \times 2.5-mm area. The surface chemical composition was analyzed using an energy-dispersive X-ray spectrometer (EDS; EDAX, United States). Surface wettability with distilled water in the air was detected using an optical contact angle meter (DSA100, Kruss, Germany). In addition, a solution containing 1% bovine serum albumin (BSA; Sigma-Aldrich, United States) was prepared, and the protein adsorption capacity of the surface of the three samples was measured using MicroBCA assay.

2.2 Macrophage polarization

Raw264.7 cells were seeded on the surface of each sample (1×10^4 cells/well). After 1, 3, and 9 days, macrophages were fixed with the Gluta fixative, dehydrated with graded ethanol, ion sputtered, and then observed using the FE-SEM (Hitachi S-4800, Japan). For each group of samples, 5 fields of view were selected at 3, 6, 9, and 12 o'clock in the center and around the samples. The spread area and longest diameter of the macrophages were measured using ImageJ software. In addition, F-actin was stained using phalloidin-Alexa Fluor 488 (1:1,000; C2201S, Beyotime, China) and incubated for 30 min, followed by incubation in mounting medium with DAPI (ab104139, Abcam, United States) and was visualized using the Olympus FV3000 confocal microscope. The cell proliferation activity of the three groups of samples was detected using the CCK-8 method.

After 7 days, the expression of M1 markers (*Mhc2*, *Inos*, and *Il-6*) and M2 markers (*Cd163* and *Cd206*) was evaluated using qRT-PCR. Primer sequences are shown in Supplementary Table S1. The TNF- α level in the cell culture was detected using an ELISA kit (EK0527, Boster, China). Meanwhile, the expression of M1 markers (iNOS and CD86) and M2 markers (CD163, CD206, and Arg-1) was evaluated using Western blot. Antibodies and dilutions included anti-CD86 (1:200; ab112490, Abcam, United States), anti-iNOS (1:1,000; ab178945, Abcam, United States), anti-CD206 (1:1,000; ab64693, Abcam, United States), anti-CD163 (1:1,000; ab182422, Abcam, United States), and anti-ARG1 (1:5,000; ab233548, Abcam, United States). The anti- β -actin antibody (1:5,000, ab6276, Abcam, United States) was used for quantifying the loading amount of the sample. In addition, the expression of M2 polarization markers

(CD206 and CD163) was observed by immunofluorescence. Antibodies and dilutions included anti-CD206 (1:500; ab64693, Abcam, United States) and anti-CD163 (1:1,000; ab182422, Abcam, United States). All stained samples were visualized using the Olympus FV3000 confocal microscope.

2.3 Osteogenesis *in vitro*

To mimic the microenvironment of bone regeneration, the MC3T3-E1 pre-osteoblasts were cultured on the three silicon surfaces and stimulated by the supernatant from macrophages cultured on the corresponding surfaces (Figure 5A). On day 7 after stimulation, the expression of osteogenic genes (*Alpl*, *Col1a1*, and *Runx2*) was detected by qRT-PCR. The alkaline phosphatase (ALP) activity was analyzed using the alkaline phosphatase activity detection kit (Beyotime, P0321S). In addition, tetracycline solution (ML6401, Mlbio, China) was added at a ratio of 1:100 to the culture medium. At 14 days, Ob fixing solution was added after PBS washing, and DAPI staining solution was added. Given that tetracycline can selectively integrate with new bone hydroxyapatite calcium (Wang et al., 2006; Sakai et al., 2010; Sordi et al., 2021), the fluorescence intensity of tetracycline was observed under a fluorescence microscope. At 21 days, 2% Alizarin Red S Staining Solution (C0138, Beyotime, China) was used to quantify deposited mineral nodules. Then, the mineralized matrix stained with Alizarin Red was destained with 10% cetylpyridinium chloride (Sigma-Aldrich) in 10 mM sodium phosphate (pH 7.0; Sigma-Aldrich), and the calcium concentration was determined using a spectrophotometer (Thermo Fisher Scientific) at 562 nm, with a standard calcium curve in the same solution.

In addition, the supernatant of the macrophages cultured on the three silicon surfaces was also used as the stimulant for rat bone marrow mesenchymal stem cells (rBMSCs). On day 3 after stimulation, ALP staining (C3206, Beyotime, China) and the expression of osteogenic proteins (RUNX2, ALPL, and OPN) were detected. Antibodies include anti-RUNX2 (1:1,000; D1L7F, Cell Signaling Technology, United States), anti-ALPL (1:1,000; 11187-1-AP, Proteintech, China), and anti-OPN (1:1,000; 22952-1-AP, Proteintech, China). The anti- β -actin antibody (1:5,000; ab6276, Abcam, United States) was used for quantifying the loading amount of the sample.

2.4 Bone regeneration *in vivo*

The calvaria of mice was selected as the animal model for *in vivo* osteogenesis evaluation (Wancket, 2015). To examine the bone regeneration effect of the Smo, Regu, and Fore surfaces, 54 male mice (8 weeks old) were selected and randomly divided into three groups under the ethical approval of the Biomedical Ethics Committee of Medical College, Xi'an Jiaotong University (No. 2021-1563). A 4-mm diameter critical-sized bone defect was created in the parietal bone of each mouse using an annulated bit. Each defect was subsequently filled with Smo, Regu, or Fore samples. For sample harvesting, the animals were euthanized with a lethal dose of pentobarbital sodium. The mouse craniums were collected and fixed in 10% formaldehyde for 72 h at room temperature. The samples were scanned by micro-CT (Y.Cheetah, YXLON, Germany). Two-dimensional slices with an isotropic resolution of

19 μm were generated and used for three-dimensional reconstruction. First, we reconstructed the three-dimensional images with the whole sample, including the silicon samples and mouse craniums. Next, a threshold was applied to the images to segment the silicon from the background, and the same threshold was used for all samples. A 4.5-mm-diameter round region of interest (ROI) centered around the epicenter of the defect was analyzed. After setting a determinate threshold, the new bone volume fraction (bone volume/total volume, BV/TV) and trabecular thickness (tb.th) were obtained.

After micro-CT analysis, the craniums were decalcified in 9% formic acid, and then, the implants were removed gently from the craniums. The decalcified craniums were dehydrated in gradient ethanol, embedded in paraffin, cut into slices, and stained with H&E. The obtained sections were also dewaxed in xylene, hydrated in gradient ethanol, incubated in 0.3% hydrogen peroxide, blocked with 1% goat serum (Sigma-Aldrich, United States), and incubated with RANKL (anti-RANKL antibody, 1:200, Abcam, ab216484). Examination and analysis were performed in blind.

2.5 Statistical analysis

Data on biological experiments were obtained from at least three parallel experiments and presented as the mean \pm standard deviation. The animals were randomly grouped before surgical treatment. Statistical differences were determined using one-way ANOVA with Tukey's *post hoc* test.

3 Results

3.1 Surface characterization

As shown in Figure 2A, the Regu silicon surface presented cylindrical pillars with uniform spacing, while the Fore silicon surface presented pillars with irregular shape and space. No representative submicron feature appeared on the Smo silicon surface. The average top surface area (Figure 2B) and maximum diameter (Figure 2C) of the pillars in Regu and Fore surfaces showed no statistical difference. The dominant element of the three samples was silicon (Figure 2D). Atomic force microscopy (Figure 2E) revealed that the surface roughness parameters (S_a , S_q , and S_z) of the Fore surface were increased compared to the Regu and Smo surfaces (Figures 2F–H). In addition, the Fore surface showed enhanced protein adsorption (Figure 2I) and hydrophilicity (Figure 2J).

3.2 Promoted macrophage M2 polarization on the Fore surface

The morphology of macrophages cultured on the three surfaces was observed first (Figure 3A). At 1 day after seeding, macrophages on the Smo and Fore surfaces fused. After 3 days, these macrophages on the Smo and Fore surfaces elongated and connected *via* pseudopodia. This trend was more notable after 9 days. On the other hand, macrophages on the Regu surface remained relatively round in shape, which implied the characteristics of colonization. Quantifications of the cell length (Figure 3B) and spread area (Figure 3C) showed significant differences

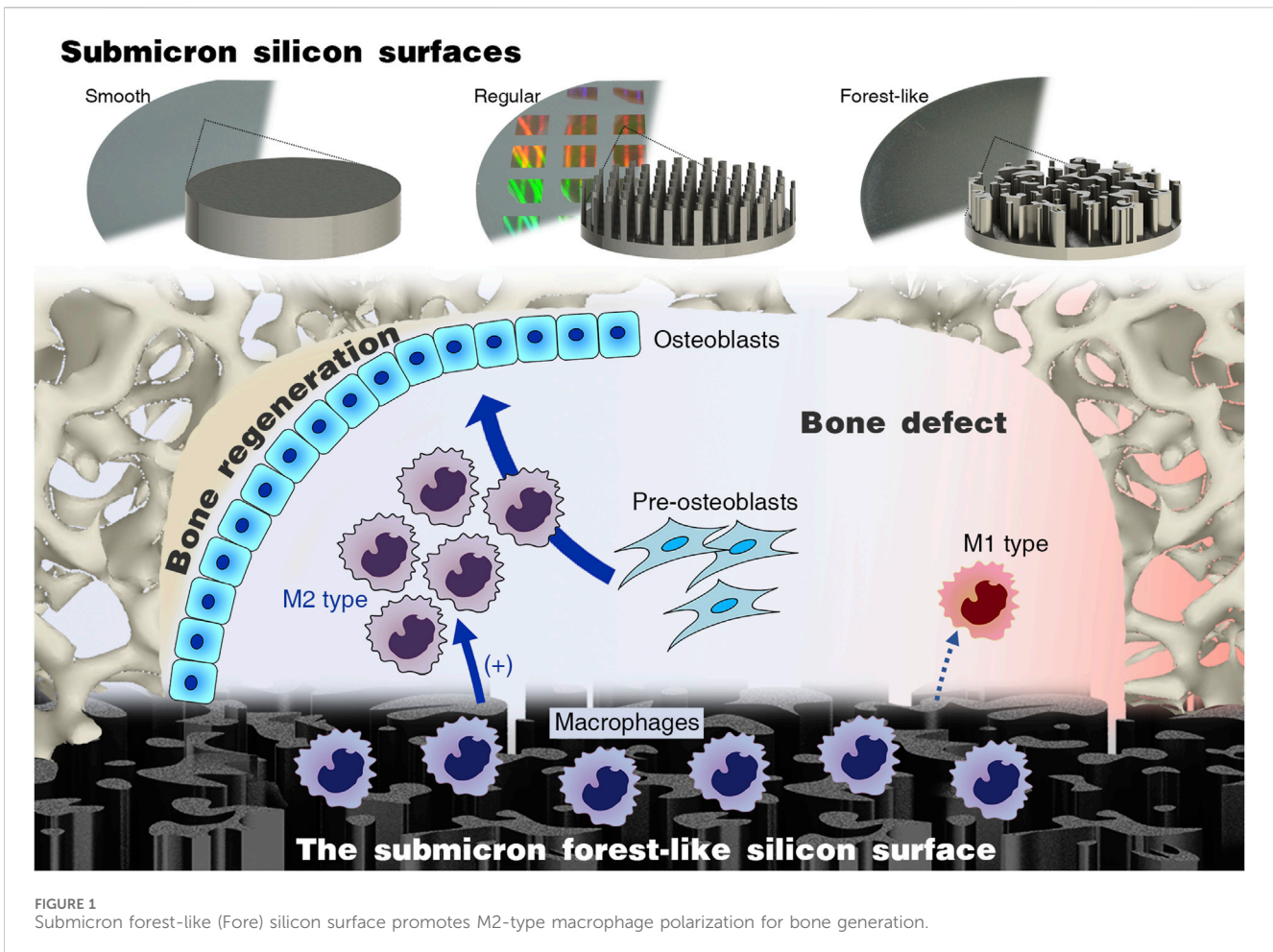


FIGURE 1
Submicron forest-like (Fore) silicon surface promotes M2-type macrophage polarization for bone generation.

between the three groups. Therefore, the Fore surface showed a significantly higher cell length and spread area. The observation obtained by confocal microscopy (Figure 3D) confirmed this trend. Moreover, the proliferation of macrophages cultured on the Fore surface increased 9 days after seeding (Figure 3E).

qRT-PCR showed that the mRNA expression level of M1 polarization markers (*Mhc2*, *Inos*, and *Il-6*) in the Fore group was significantly decreased, while the mRNA expression level of M2 polarization markers (CD163 and CD206) was significantly increased (Figure 4A). At the same time, the levels of TNF- α secreted by Raw264.7 cells on the surface of Fore samples were significantly reduced (Figure 4B). The immunofluorescence intensity of CD163 and CD206 in the Fore group was significantly enhanced, with statistical differences (Figures 4C, D). This trend was also verified using Western blot (Figure 4E) that the protein expression of M2 polarization factors (CD206, CD163, and Arg-1) on the Fore sample increased significantly, and the protein expression of M1 polarization factors (CD86 and iNOS) decreased significantly.

3.3 Enhanced *in vitro* osteogenesis on the Fore surface

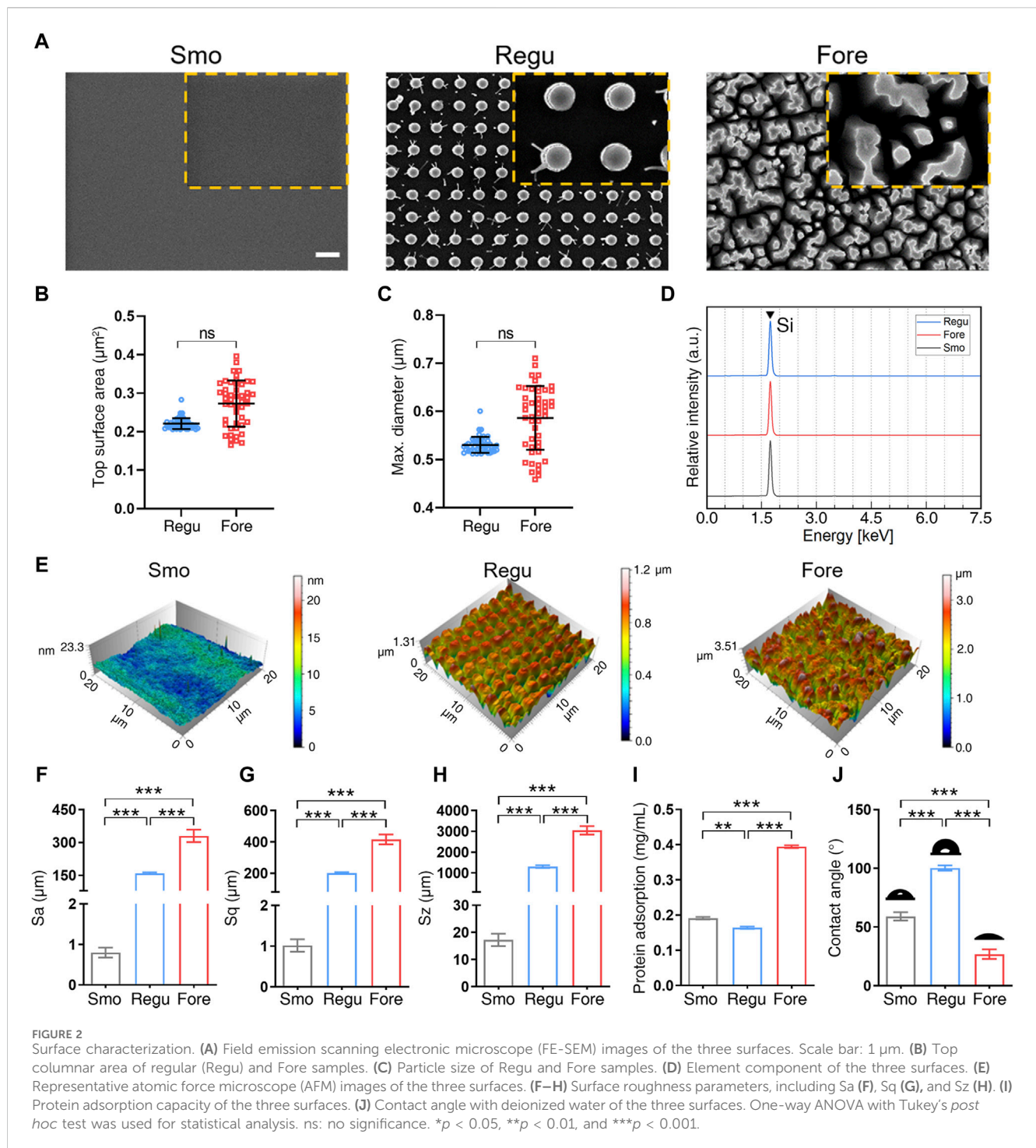
After being stimulated by the supernatant from macrophages cultured on corresponding surfaces (Figure 5A), the expression of

osteogenic genes (*Alpl*, *Col1a1*, and *Runx2*) of MC3T3-E1 cells in the Fore + RAW group increased significantly on day 7 (Figure 5B). At the same time, the ALP activity in the Fore + RAW group was significantly higher (Figure 5C). The promotion of osteogenesis was also observed by immunofluorescence by tetracycline staining in the Fore + RAW group at 14 days (Figure 5D, E). Similar trends were also found in the staining of Alizarin Red S at 21 days (Figure 5F and Supplementary Figure S1), with more mineral nodules in the Fore + RAW group.

In rBMSCs stimulated by the supernatant from macrophages cultured on the three silicon surfaces (Figure 5G), the alkaline phosphatase activity (Figure 5H) and the expression of RUNX2, ALPL, and OPN (Figure 5I) were increased significantly. Overall, these results proved that the immune microenvironment of the Fore surface could promote bone formation.

3.4 Promoted *in vivo* bone regeneration on the Fore surface

As shown in Figure 6A, the bone regeneration was investigated with a round (Φ 4 mm) bone defect on the mouse calvaria. At 4 weeks post-implantation, a new bone began to form on the edge of the bone defect in all 3 groups, and at 8 weeks and 12 weeks, the new bone on the surface of Fore samples was significantly higher than those in Smo and Regu samples, respectively (Figures 6B–D). Histological analysis



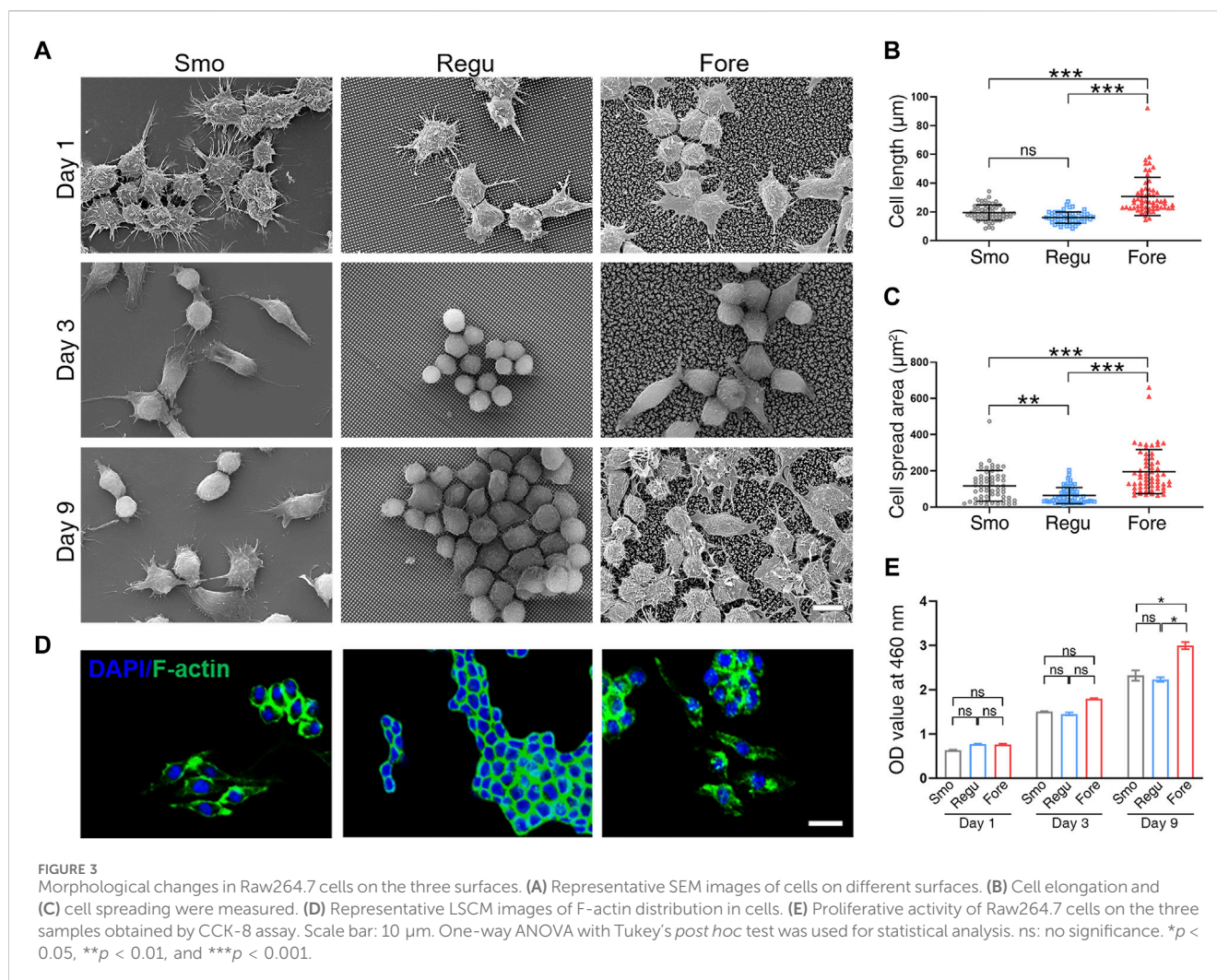
of the heart, liver, spleen, lung, and kidney at 12 weeks confirmed good biosafety of all Smo, Regu, and Fore specimens (Supplementary Figure S2). At 12 weeks, the expression level of RANKL in the new bone on the Fore surface decreased significantly (Figures 6E, F).

4 Discussion

In this study, a submicron forest-like silicon surface was proposed to verify whether its irregular distribution of silicon

pillars on biomaterials can promote bone regeneration. The result showed enhanced macrophage M2 polarization and succedent osteogenesis *in vitro* and promoted bone defect closure *in vivo* compared with the submicron regular and smooth silicon surfaces. Therefore, the irregular forest-like submicron pillar is a potential design for developing silicon-based bone healing biomaterials.

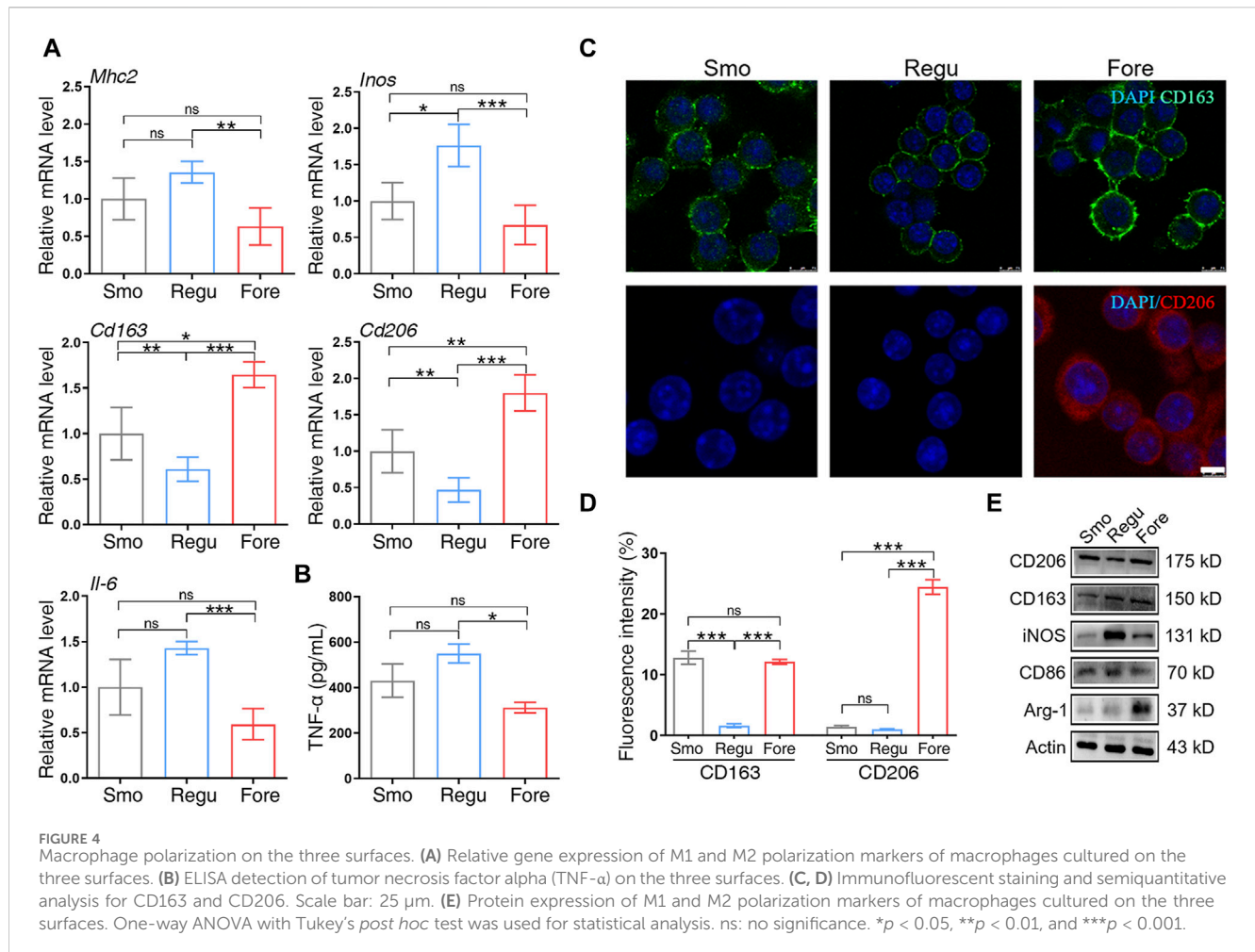
Human bone is a complex multi-scale hierarchical structure (Reznikov et al., 2014). Therefore, varied surface topographies at the micron, submicron, and nano-scales are developed in current intrabony implants (Shah et al., 2019) and are closely related to



bone regeneration. It has been well documented that the micron topography facilitates the mechanical anchorage between bone and biomaterials, while the nano-topography offers more adhesion positions for proteins at the early stage of bone regeneration (Albrektsson and Wennerberg, 2019). However, the significance of submicron topography has not been clearly defined yet. A typical submicron topography is sandblasted and acid-etched (SLA) pits on titanium implants, which is the dominant surface topography in dental implants (Smeets et al., 2016). The SLA implants have shown a less than 5% failure rate at 10 years post-implantation (Albrektsson and Wennerberg, 2019), which implies the positive effect of submicron surface topography in biomaterials on bone regeneration. In this study, the irregularly distributed Fore structure showed higher potential in stimulating the M2 polarization of macrophages and osteogenesis of pre-osteoblasts. This finding is an important supplement to the correlation with surface topography and macrophage polarization. The forest-like silicon surface shows a larger pore size and more abundant porous structure than the regular silicon pillar surface, which may explain the better anti-inflammatory activity and osteogenesis potential (Garg et al., 2013; Rustom et al., 2019). The Fore surface was more hydrophilic than the Regu surface (Figure 2)). Macrophages adhered to a hydrophilic

surface tend to enhance the secretion of anti-inflammatory cytokines and M2 surface markers (Hotchkiss et al., 2016; Lv et al., 2018). In addition, it is found that the “topographical effect” plays important roles in macrophage behavior and osteogenesis (Ma et al., 2014; Wang J. et al., 2018). Sa, Sq, and Sz may influence the anti-inflammatory activity and osteogenesis potential. Overall, the result of this study echoes the current opinion that material surfaces resembling the natural bone structure are beneficial to osteogenesis (Boyan et al., 2017; Shah et al., 2019; Berger et al., 2022).

To date, titanium-based implants are holding the largest market share in tooth and bone restoration (Kaur and Singh, 2019). However, the biocompatibility of titanium is gradually being questioned due to inflammatory reactivity or metal hypersensitivity in some patients (Buettner and Valentine, 2012). Further improvement of surface biocompatibility is pivotal in developing the next generation of intrabony implants (Bandyopadhyay et al., 2023). Silicon, as a major trace element in humans (Martin, 2013), shows relatively stable *in vivo* metabolism (Jugdaohsingh et al., 2013). Wang et al. (2023) prepared silicon-deposited coatings on Ti-based implants via electron beam evaporation (Wang et al., 2023), which showed osteoinductive and immunomodulatory capacity. It was found that the burst



release of Si dominated the early stages of implantation to create a favorable osteoimmunomodulatory microenvironment by the timely conversion of macrophages from an M1 to an M2 phenotype that facilitated osteogenic differentiation. In addition, the release of Si also directly activated stem cells and remodeled the extracellular matrix for late osseointegration. For instance, Francesco et al. increased the surface porosity and biological activity of the implants by embedding Si_3N_4 particles on the surface of PEEK implants (Boschetto et al., 2021), which showed the advantages of a low elastic modulus, improved bone integration, and promoted antibacterial effects. At the same time, a porous scaffold based on a Fe-Si alloy was manufactured by 3D printing technology, which could reduce cytotoxicity and improve mechanical stability and bone integration ability (Bondareva et al., 2022). Similar findings have been made in other implants, for example, Edward et al. found that mechanically matched silicone brain implants could potentially improve the long-term functionality and reliability of brain implants by minimizing strain and stress due to movements and swelling of the brain in both lateral and axial directions relative to the implant (E. Zhang D. H. et al., 2021). The result of this study further suggests that irregular submicron silicon surfaces are better than regular submicron silicon surfaces in bone regeneration, which is important for fabricating and optimizing future silicon-based biomaterials.

In addition, the fate of macrophages can be regulated by the surface topography of biomaterials (Hotchkiss et al., 2016; Abaricia et al., 2020; Zhu G. et al., 2021). Existing studies have confirmed that the shape and polarization of macrophages can be influenced by nanotopography of biomaterials (Ma et al., 2014; Neacsu et al., 2014; Wang J. et al., 2018). Nanotubes with a larger diameter are prone to induce M2 polarization of macrophages (Lü et al., 2015; Xu et al., 2019; Yu et al., 2021). The result of this study supports that submicron morphologies at the range of 250–500 nm can also manipulate macrophage polarization, which is an important supplement to current theories.

The control of immune responses after biomaterial implantation in the body has long been a concern in the development of medical implants (Naik et al., 2018). The increase in the number of M2-like macrophages in the damaged tissue has been suggested to be an essential event in tissue healing. Delayed polarization from the inflammatory M1 phenotype into the anti-inflammatory/healing M2 phenotype would lead to compromised stem/progenitor cell response to inhibit the functional regeneration of skin, muscle, heart, nerve, and bone (Zhang E. N. et al., 2021; Li et al., 2021). In this proof-of-concept report using bone as a model tissue, we demonstrate tissue-biomaterial integration in

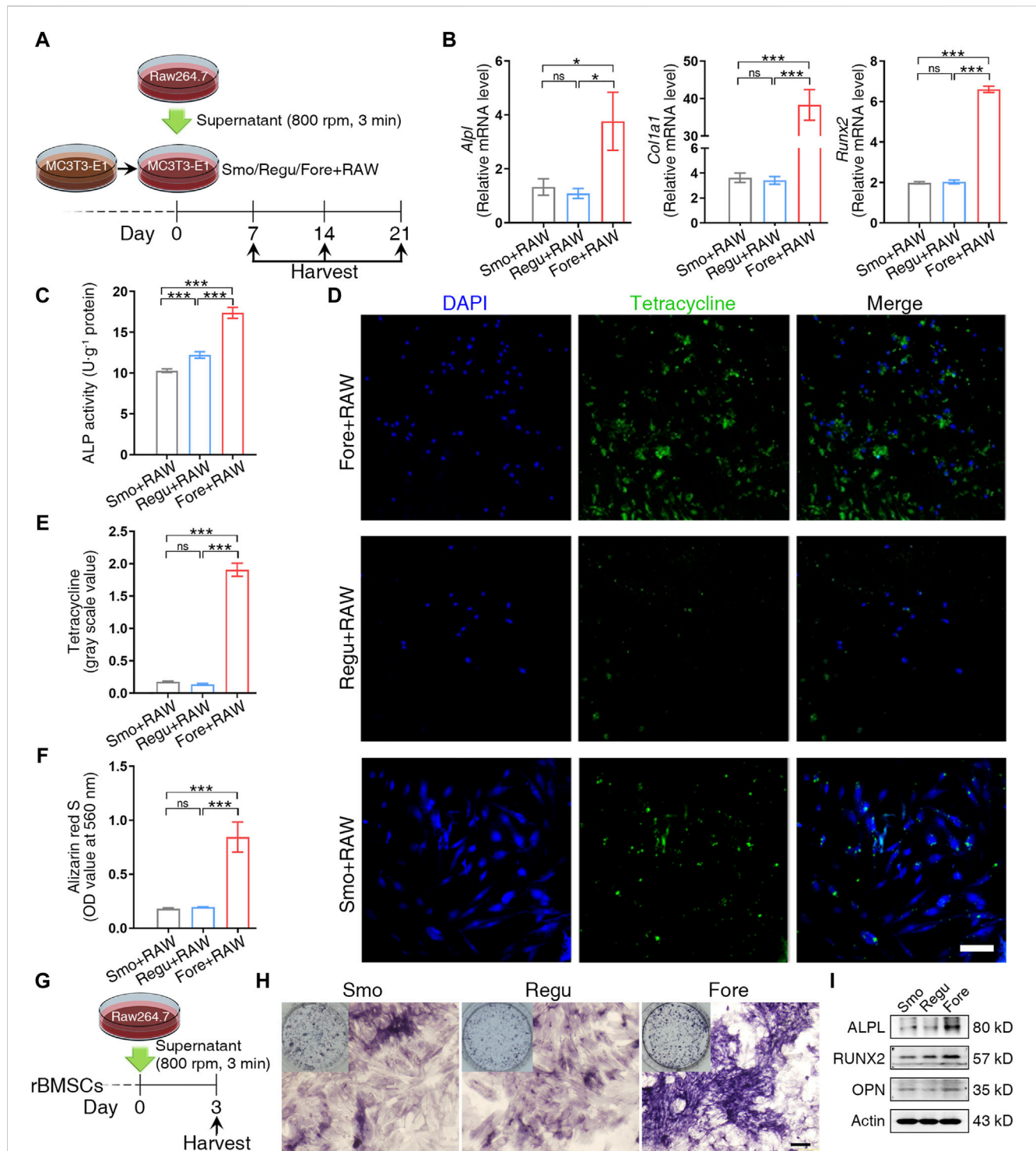
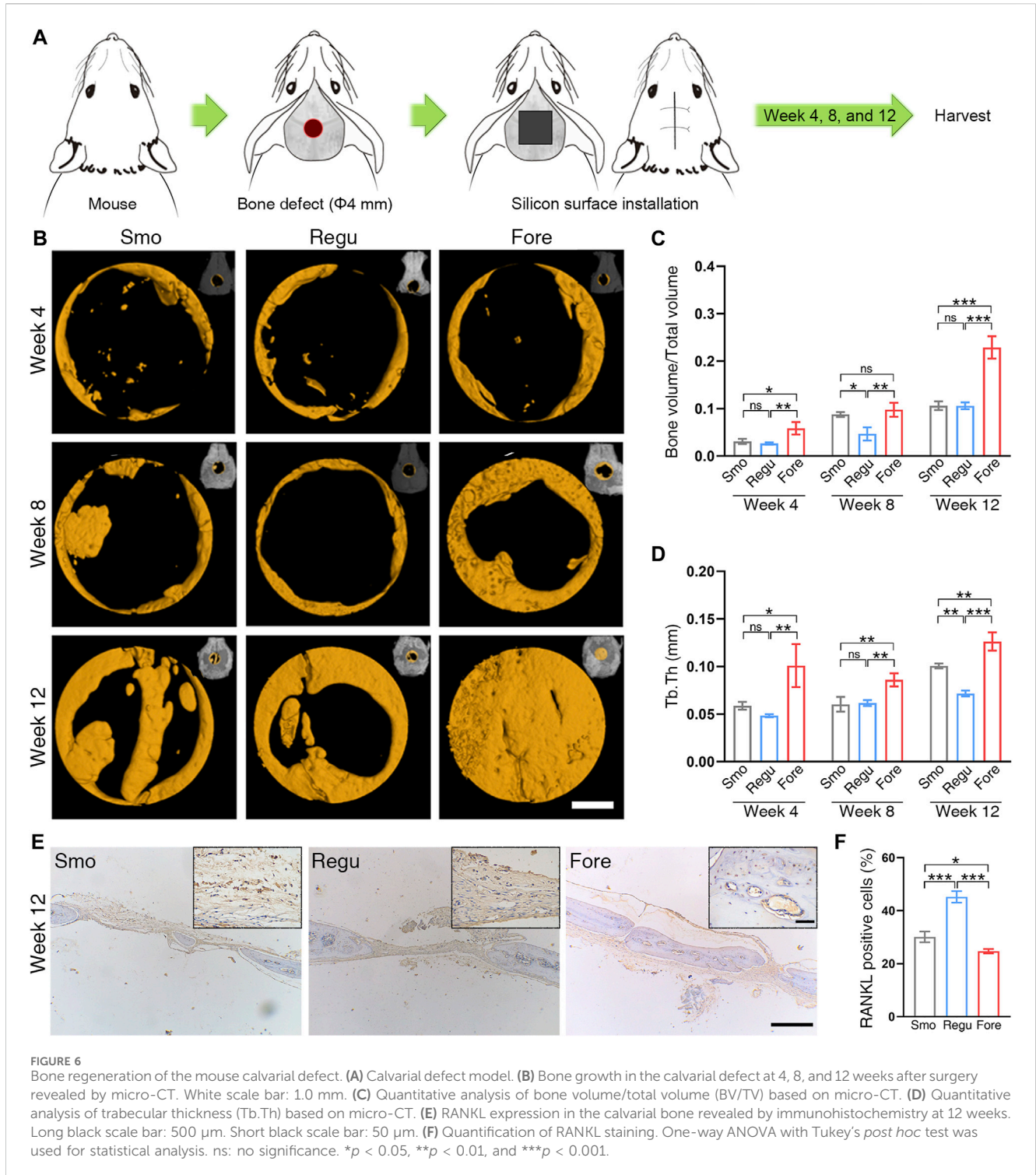


FIGURE 5
Cell osteogenic differentiation on the surface of the three samples. **(A)** Schematic diagram of MC3T3-E1 cell management. **(B)** Relative gene expression of osteogenic genes of MC3T3-E1 cells cultured on the three surfaces on day 7. **(C)** Alkaline phosphatase (ALP) activity of MC3T3-E1 cells cultured on the three surfaces on day 7. **(D, E)** Tetracycline distribution in MC3T3-E1 cells cultured on the three surfaces and semiquantitative analysis on day 14. White scale bar: 100 μm. **(F)** Semiquantification of the calcium nodule formation evaluation by Alizarin Red staining on day 21. **(G)** Schematic diagram of rat bone marrow mesenchymal stem cell (rBMSCs) management. **(H)** ALP activity staining. Black scale bar: 200 μm. **(I)** Protein expression of osteogenic markers. One-way ANOVA with Tukey's *post hoc* test was used for statistical analysis. ns: no significance. **p* < 0.05, ***p* < 0.01, and ****p* < 0.001.



irregular forest-like submicron silicon-based coating with the concurrent modulation of the macrophage response and cytokine profile manifested in the M2-based phenotype. This phenotype switching is pivotal in improving tissue regeneration induced by biomaterials (Huyer et al., 2020; Schlundt et al., 2021). Osteoclasts play a key role in the process of bone regeneration, and RANKL (ligand), expressed by osteoblasts and bone marrow stromal cells, attaches to RANK receptors on mature osteoclasts and osteoclast

progenitor cells and promotes their differentiation (Shah et al., 2018; Huntley et al., 2019). In addition to inducing osteoclast activity, RANKL also induces osteoclasts to attach to the bone surface and longevity (Chaparro et al., 2022). In this study, we evaluated the expression of RANKL in the new bone and found that RANKL expression decreased significantly in the Fore group while increased significantly in the Regu group, which was consistent with the results of bone regeneration.

5 Conclusion

In this study, an irregular forest-like submicron silicon surface was proposed as a promising design of biomaterials for bone regeneration. It demonstrated better *in vitro* and *in vivo* biological responses than the regular submicron silicon surface and smooth silicon surface, including promoting macrophage M2 polarization and facilitating bone formation. This finding enriches the research basis for silicon-based biomaterials and highlights the irregular surface design for better bone regeneration performance.

Data availability statement

The datasets presented in this study can be found in online repositories. The names of the repository/repositories and accession number(s) can be found in the article/[Supplementary Material](#).

Ethics statement

The animal study was approved by the Biomedical Ethics Committee of Medical College, Xi'an Jiaotong University. The study was conducted in accordance with the local legislation and institutional requirements.

Author contributions

GS: conceptualization, investigation, methodology, formal analysis, and writing—original draft. TS: funding acquisition, software, visualization, writing—review and editing. SM: writing—review and editing. ML: writing—review and editing. ZQ: conceptualization, funding acquisition, resources, project administration, supervision, validation, writing—review and editing. AL: conceptualization, funding acquisition, resources, project administration, supervision, validation, writing—review and editing.

Funding

The author(s) declare that financial support was received for the research, authorship, and/or publication of this article. The

References

- Abaricia, J. O., Shah, A. H., Chaubal, M., Hotchkiss, K. M., and Olivares-Navarrete, R. (2020). Wnt signaling modulates macrophage polarization and is regulated by biomaterial surface properties. *Biomaterials* 243, 119920. doi:10.1016/j.biomaterials.2020.119920
- Akasaka, T., Tamai, M., Yoshimura, Y., Ushijima, N., Numamoto, S., Yokoyama, A., et al. (2022). Different micro/nano-scale patterns of surface materials influence osteoclastogenesis and actin structure. *Nano Res.* 15 (5), 4201–4211. doi:10.1007/s12274-021-4026-3
- Albrektsson, T., and Wennerberg, A. (2019). On osseointegration in relation to implant surfaces. *Clin. Implant Dent. Relat. Res.* 21 (Suppl. 1), 4–7. doi:10.1111/cid.12742
- Angeloni, L., Popa, B., Nouri-Goushki, M., Minneboo, M., Zadpoor, A. A., Ghatkesar, M. K., et al. (2023). Fluidic force microscopy and atomic force microscopy unveil new insights into the interactions of preosteoblasts with 3D-printed submicron patterns. *Small* 19 (2), e2204662. doi:10.1002/smll.202204662
- Bai, X., Gao, M., Syed, S., Zhuang, J., Xu, X., and Zhang, X. Q. (2018). Bioactive hydrogels for bone regeneration. *Bioact. Mat.* 3 (4), 401–417. doi:10.1016/j.bioactmat.2018.05.006
- Bandyopadhyay, A., Mitra, I., Goodman, S. B., Kumar, M., and Bose, S. (2023). Improving biocompatibility for next generation of metallic implants. *Prog. Mat. Sci.* 133, 101053. doi:10.1016/j.pmatsci.2022.101053
- Berger, M. B., Slosar, P., Schwartz, Z., Cohen, D. J., Goodman, S. B., Anderson, P. A., et al. (2022). A review of biomimetic topographies and their role in promoting bone formation and osseointegration: implications for clinical use. *Biomimetics* 7 (2), 46. doi:10.3390/biomimetics7020046
- Bock, R. M., Jones, E. N., Ray, D. A., Sonny Bal, B., Pezzotti, G., and McEntire, B. J. (2017). Bacteriostatic behavior of surface modulated silicon nitride in comparison to polyetheretherketone and titanium. *J. Biomed. Mat. Res. A* 105 (5), 1521–1534. doi:10.1002/jbm.a.35987

author acknowledges the support by the Innovative Research Groups of the National Natural Science Foundation of China (51721004), the National Natural Science Foundation of China (82071078), the Natural Science Foundation of Shaanxi Province (2023-JC-QN-0842), the Fundamental Research Funds for the Central Universities, Xi'an Jiaotong University (xtr012019007, xzy022022071), the Opening Research Fund from the Key Laboratory of Shaanxi Province for Craniofacial Precision Medicine Research, College of Stomatology, Xi'an Jiaotong University (2021LHM-KFKT001), and the Transdisciplinary Support Project for PhD, Xi'an Jiaotong University (IDT1721).

Acknowledgments

The authors acknowledge Suzhou Research Materials Microtech Co., Ltd. for their assistance in the preparation of silicon samples.

Conflict of interest

The authors declare that the research was conducted in the absence of any commercial or financial relationships that could be construed as a potential conflict of interest.

Publisher's note

All claims expressed in this article are solely those of the authors and do not necessarily represent those of their affiliated organizations, or those of the publisher, the editors, and the reviewers. Any product that may be evaluated in this article, or claim that may be made by its manufacturer, is not guaranteed or endorsed by the publisher.

Supplementary material

The Supplementary Material for this article can be found online at: <https://www.frontiersin.org/articles/10.3389/fbioe.2024.1356158/full#supplementary-material>

- Bondareva, J. V., Dubinin, O. N., Kuzminova, Y. O., Shpichka, A. I., Kosheleva, N. V., Lychagin, A. V., et al. (2022). Biodegradable iron-silicon implants produced by additive manufacturing. *Biomed. Mat.* 17 (3), 035005. doi:10.1088/1748-605X/ac6124
- Boschetto, F., Marin, E., Ohgiani, E., Adachi, T., Zanocco, M., Horiguchi, S., et al. (2021). Surface functionalization of PEEK with silicon nitride. *Biomed. Mat.* 16 (1), 015015. doi:10.1088/1748-605X/abb6b1
- Bosshardt, D. D., Chappuis, V., and Buser, D. (2017). Osseointegration of titanium, titanium alloy and zirconia dental implants: current knowledge and open questions. *Periodontol* 73 (1), 22–40. doi:10.1111/prd.12179
- Boyan, B. D., Lotz, E. M., and Schwartz, Z. (2017). Roughness and hydrophilicity as osteogenic biomimetic surface properties. *Tissue Eng. Part A* 23 (23–24), 1479–1489. doi:10.1089/ten.TEA.2017.0048
- Brown, M. A., Zappitelli, K. M., Singh, L., Yuan, R. C., Bemrose, M., Brogden, V., et al. (2023). Direct laser writing of 3D electrodes on flexible substrates. *Nat. Comm.* 14 (1), 3610. doi:10.1038/s41467-023-39152-7
- Buettner, K. M., and Valentine, A. M. (2012). Bioinorganic chemistry of titanium. *Chem. Rev.* 112 (3), 1863–1881. doi:10.1021/cr1002886
- Chaparro, A., Beltrán, V., Betancur, D., Sam, Y.-H., Moaven, H., Tarjomani, A., et al. (2022). Molecular biomarkers in peri-implant health and disease: a cross-sectional pilot study. *Int. J. Mol. Sci.* 23 (17), 9802. doi:10.3390/ijms23179802
- Chen, Z., Klein, T., Murray, R. Z., Crawford, R., Chang, J., Wu, C., et al. (2016). Osteoimmunomodulation for the development of advanced bone biomaterials. *Mat. Today* 19 (6), 304–321. doi:10.1016/j.mattod.2015.11.004
- Du, X., Lee, S. S., Blugan, G., and Ferguson, S. J. (2022). Silicon nitride as a biomedical material: an overview. *Int. J. Mol. Sci.* 23 (12), 6551. doi:10.3390/ijms23126551
- Friguglietti, J., Das, S., Le, P., Fraga, D., Quintela, M., Gazze, S. A., et al. (2020). Novel silicon titanium diboride micropatterned substrates for cellular patterning. *Biomaterials* 244, 119927. doi:10.1016/j.biomaterials.2020.119927
- Ganjian, M., Modaresifar, K., Rompolas, D., Fratila-Apachitei, L. E. E., and Zadpoor, A. A. A. (2022). Nanoimprinting for high-throughput replication of geometrically precise pillars in fused silicon dioxide to regulate cell behavior. *Acta Biomater.* 140, 717–729. doi:10.1016/j.actbio.2021.12.001
- Garg, K., Pullen, N. A., Oskertizian, C. A., Ryan, J. J., and Bowlin, G. L. (2013). Macrophage functional polarization (M1/M2) in response to varying fiber and pore dimensions of electrospun scaffolds. *Biomaterials* 34 (18), 4439–4451. doi:10.1016/j.biomaterials.2013.02.065
- Hotchkiss, K. M., Reddy, G. B., Hyzy, S. L., Schwartz, Z., Boyan, B. D., and Olivares-Navarrete, R. (2016). Titanium surface characteristics, including topography and wettability, alter macrophage activation. *Acta Biomater.* 31, 425–434. doi:10.1016/j.actbio.2015.12.003
- Huntley, R., Jensen, E., Gopalakrishnan, R., and Mansky, K. C. (2019). Bone morphogenetic proteins: their role in regulating osteoclast differentiation. *Bone Rep.* 10, 100207. doi:10.1016/j.bonr.2019.100207
- Huyer, L. D., Pascual-Gil, S., Wang, Y. F., Mandla, S., Yee, B., and Radisic, M. (2020). Advanced strategies for modulation of the material-macrophage interface. *Adv. Funct. Mat.* 30 (44), 1909331. doi:10.1002/adfm.201909331
- Ishikawa, M., de Mesy Bentley, K. L., McEntire, B. J., Bal, B. S., Schwarz, E. M., and Xie, C. (2017). Surface topography of silicon nitride affects antimicrobial and osseointegrative properties of tibial implants in a murine model. *J. Biomed. Mat. Res. A* 105 (12), 3413–3421. doi:10.1002/jbm.a.36189
- Jugdaohsingh, R., Sripanyakorn, S., and Powell, J. J. (2013). Silicon absorption and excretion is independent of age and sex in adults. *Brit. J. Nutr.* 110 (6), 1024–1030. doi:10.1017/S0007114513000184
- Jugdaohsingh, R., Tucker, K. L., Qiao, N., Cupples, L. A., Kiel, D. P., and Powell, J. J. (2004). Dietary silicon intake is positively associated with bone mineral density in men and premenopausal women of the Framingham Offspring cohort. *J. Bone Min. Res.* 19 (2), 297–307. doi:10.1359/jbmr.0301225
- Kaur, M., and Singh, K. (2019). Review on titanium and titanium based alloys as biomaterials for orthopaedic applications. *Mat. Sci. Eng. C* 102, 844–862. doi:10.1016/j.msec.2019.04.064
- Kooy, N., Mohamed, K., Pin, L. T., and Guan, O. S. (2014). A review of roll-to-roll nanoimprint lithography. *Nanoscale Res. Lett.* 9, 320. doi:10.1186/1556-276x-9-320
- Li, J. H., Jiang, X. Q., Li, H. J., Gelinsky, M., and Gu, Z. (2021). Tailoring materials for modulation of macrophage fate. *Adv. Mat.* 33 (12), 2004172. doi:10.1002/adma.202004172
- Lü, W. L., Wang, N., Gao, P., Li, C. Y., Zhao, H. S., and Zhang, Z. T. (2015). Effects of anodic titanium dioxide nanotubes of different diameters on macrophage secretion and expression of cytokines and chemokines. *Cell Prolif.* 48 (1), 95–104. doi:10.1111/cpr.12149
- Lv, L., Xie, Y., Li, K., Hu, T., Lu, X., Cao, Y., et al. (2018). Unveiling the mechanism of surface hydrophilicity-modulated macrophage polarization. *Adv. Healthc. Mat.* 7 (19), 1800675. doi:10.1002/adhm.201800675
- Ma, Q. L., Zhao, L. Z., Liu, R. R., Jin, B. Q., Song, W., Wang, Y., et al. (2014). Improved implant osseointegration of a nanostructured titanium surface via mediation of macrophage polarization. *Biomaterials* 35 (37), 9853–9867. doi:10.1016/j.biomaterials.2014.08.025
- Martin, K. R. (2013). Silicon: the health benefits of a metalloid. *Metall. Ions Life Sci.* 13, 451–473. doi:10.1007/978-94-007-7500-8_14
- Naik, S., Larsen, S. B., Cowley, C. J., and Fuchs, E. (2018). Two to tango: dialog between immunity and stem cells in health and disease. *Cell* 175 (4), 908–920. doi:10.1016/j.cell.2018.08.071
- Neacsu, P., Mazare, A., Cimpean, A., Park, J., Costache, M., Schmuki, P., et al. (2014). Reduced inflammatory activity of RAW 264.7 macrophages on titania nanotube modified Ti surface. *Int. J. Biochem. Cell Biol.* 55, 187–195. doi:10.1016/j.biocel.2014.09.006
- Nouri-Goushki, M., Isaakidou, A., Eijkel, B. I. M., Minneboo, M., Liu, Q., Boukany, P. E., et al. (2021). 3D printed submicron patterns orchestrate the response of macrophages. *Nanoscale* 13 (34), 14304–14315. doi:10.1039/d1nr01557e
- Nouri-Goushki, M., Mirzaali, M. J., Angeloni, L., Fan, D., Minneboo, M., Ghatkesar, M. K., et al. (2020). 3D printing of large areas of highly ordered submicron patterns for modulating cell behavior. *ACS Appl. Mat. Interfaces* 12 (1), 200–208. doi:10.1021/acsmi.9b17425
- Reznikov, N., Shahar, R., and Weiner, S. (2014). Bone hierarchical structure in three dimensions. *Acta Biomater.* 10 (9), 3815–3826. doi:10.1016/j.actbio.2014.05.024
- Rustom, L. E., Poellmann, M. J., and Wagoner Johnson, A. J. (2019). Mineralization in micropores of calcium phosphate scaffolds. *Acta Biomater.* 83, 435–455. doi:10.1016/j.actbio.2018.11.003
- Sakai, V. T., Zhang, Z., Dong, Z., Neiva, K. G., Machado, M. A. A. M., Shi, S., et al. (2010). SHED differentiate into functional odontoblasts and endothelium. *J. Dent. Res.* 89 (8), 791–796. doi:10.1177/0022034510368647
- Schlundt, C., Fischer, H., Bucher, C. H., Rendenbach, C., Duda, G. N., and Schmidt-Bleek, K. (2021). The multifaceted roles of macrophages in bone regeneration: a story of polarization, activation and time. *Acta Biomater.* 133, 46–57. doi:10.1016/j.actbio.2021.04.052
- Shah, F. A., Thomsen, P., and Palmquist, A. (2018). A review of the impact of implant biomaterials on osteocytes. *J. Dent. Res.* 97 (9), 977–986. doi:10.1177/0022034518778033
- Shah, F. A., Thomsen, P., and Palmquist, A. (2019). Osseointegration and current interpretations of the bone-implant interface. *Acta Biomater.* 84, 1–15. doi:10.1016/j.actbio.2018.11.018
- Smeets, R., Stadlinger, B., Schwarz, F., Beck-Broichsitter, B., Jung, O., Precht, C., et al. (2016). Impact of dental implant surface modifications on osseointegration. *Biomed. Res. Int.* 16, 1–16. doi:10.1155/2016/6285620
- Sordi, M. B., Curtarelli, R. B., da Silva, I. T., Fongaro, G., Benfatti, C. A. M., de Souza Magini, R., et al. (2021). Effect of dexamethasone as osteogenic supplementation in *in vitro* osteogenic differentiation of stem cells from human exfoliated deciduous teeth. *J. Mat. Sci.* 32 (1), 1. doi:10.1007/s10856-020-06475-6
- Sun, J. L., Jiao, K., Niu, L. N., Jiao, Y., Song, Q., Shen, L. J., et al. (2017). Intrafibrillar silicified collagen scaffold modulates monocyte to promote cell homing, angiogenesis and bone regeneration. *Biomaterials* 113, 203–216. doi:10.1016/j.biomaterials.2016.10.050
- Sun, J. L., Jiao, K., Song, Q., Ma, C. F., Ma, C., Tay, F. R., et al. (2018). Intrafibrillar silicified collagen scaffold promotes *in-situ* bone regeneration by activating the monocyte p38 signaling pathway. *Acta Biomater.* 67, 354–365. doi:10.1016/j.actbio.2017.12.022
- Toita, R., Kang, J. H., and Tsuchiya, A. (2022). Phosphatidylserine liposome multilayers mediate the M1-to-M2 macrophage polarization to enhance bone tissue regeneration. *Acta Biomater.* 154, 583–596. doi:10.1016/j.actbio.2022.10.024
- Trindade, R., Albrektsson, T., Tengvall, P., and Wennerberg, A. (2016). Foreign body reaction to biomaterials: on mechanisms for buildup and breakdown of osseointegration. *Clin. Implant Dent. Relat. Res.* 18 (1), 192–203. doi:10.1111/cid.12274
- Wancket, L. M. (2015). Animal models for evaluation of bone implants and devices: comparative bone structure and common model uses. *Vet. Pathol.* 52 (5), 842–850. doi:10.1177/0300985815593124
- Wang, J., Meng, F., Song, W., Jin, J., Ma, Q., Fei, D., et al. (2018a). Nanostructured titanium regulates osseointegration via influencing macrophage polarization in the osteogenic environment. *Int. J. Nanomedicine* 13, 4029–4043. doi:10.2147/ijn.S163956
- Wang, T., Chen, X., Zhang, Y., Ye, T., Liu, Z., Wang, L., et al. (2023). Immunoregulatory silicon-deposited implant promotes osseointegration. *Compos. Part B Eng.* 255, 110618. doi:10.1016/j.compositesb.2023.110618
- Wang, X., Wang, G., Zingales, S., and Zhao, B. (2018b). Biomaterials enabled cell-free strategies for endogenous bone regeneration. *Tissue Eng. Part B Rev.* 24 (6), 463–481. doi:10.1089/ten.TEB.2018.0012
- Wang, Y. H., Liu, Y., Maye, P., and Rowe, D. W. (2006). Examination of mineralized nodule formation in living osteoblastic cultures using fluorescent dyes. *Biotechnol. Prog.* 22 (6), 1697–1701. doi:10.1021/bp060274b
- Xu, W. C., Dong, X., Ding, J. L., Liu, J. C., Xu, J. J., Tang, Y. H., et al. (2019). Nanotubular TiO₂ regulates macrophage M2 polarization and increases macrophage

secretion of VEGF to accelerate endothelialization via the ERK1/2 and PI3K/AKT pathways. *Int. J. Nanomedicine* 14, 441–455. doi:10.2147/ijn.S188439

Yu, W. P., Ding, J. L., Liu, X. L., Zhu, G. D., Lin, F., Xu, J. J., et al. (2021). Titanium dioxide nanotubes promote M2 polarization by inhibiting macrophage glycolysis and ultimately accelerate endothelialization. *Immun. Inflamm. Dis.* 9 (3), 746–757. doi:10.1002/iid3.429

Zhang, D. H., Chen, Q., Shi, C., Chen, M. Z., Ma, K. Q., Wan, J. L., et al. (2021a). Dealing with the foreign-body response to implanted biomaterials: strategies and applications of new materials. *Adv. Funct. Mat.* 31 (6), 2007226. doi:10.1002/adfm.202007226

Zhang, E. N., Clément, J.-P., Alameri, A., Ng, A., Kennedy, T. E., and Juncker, D. (2021b). Mechanically matched silicone brain implants reduce brain foreign body response. *Adv. Mat. Technol.* 6 (3), 2000909. doi:10.1002/admt.202000909

Zhu, G., Zhang, T., Chen, M., Yao, K., Huang, X., Zhang, B., et al. (2021a). Bone physiological microenvironment and healing mechanism: basis for future bone-tissue engineering scaffolds. *Bioact. Mat.* 6 (11), 4110–4140. doi:10.1016/j.bioactmat.2021.03.043

Zhu, Y. Z., Liang, H., Liu, X. M., Wu, J., Yang, C., Wong, T. M., et al. (2021b). Regulation of macrophage polarization through surface topography design to facilitate implant-to-bone osteointegration. *Sci. Adv.* 7 (14), eabf6654. doi:10.1126/sciadv.abf6654